Drift velocity versus electric field in < 110 > Si nanowires: Strong confinement effects

Jing Li, Gabriel Mugny, Yann-Michel Niquet, Christophe Delerue

Applied Physics Letters

Drift velocity versus electric field in ⟨110⟩ Si nanowires: Strong confinement effects

Cite as: Appl. Phys. Lett. **107**, 063103 (2015); https://doi.org/10.1063/1.4928525
Submitted: 17 June 2015 • Accepted: 30 July 2015 • Published Online: 11 August 2015

Jing Li, Gabriel Mugny, Yann-Michel Niquet, et al.

AIP Publishing

Drift velocity versus electric field in ⟨110⟩ Si nanowires: Strong confinement effects

Jing Li,[1] Gabriel Mugny,[2,3,4] Yann-Michel Niquet,[1,a)] and Christophe Delerue[4,b)]
[1]*Univ. Grenoble Alpes, INAC-SP2M, L_Sim, Grenoble, France and CEA, INAC-SP2M, L_Sim, Grenoble, France*
[2]*STMicroelectronics, 850 rue J. Monnet, 38926 Crolles, France*
[3]*CEA, LETI-MINATEC, 38000 Grenoble, France*
[4]*IEMN—Dept. ISEN, UMR CNRS 8520, Lille, France*

(Received 17 June 2015; accepted 30 July 2015; published online 11 August 2015)

We have performed atomistic simulations of the phonon-limited high field carrier transport in ⟨110⟩ Si nanowires with small diameter. The carrier drift velocities are obtained from a direct solution of the non-linear Boltzmann transport equation. The relationship between the drift velocity and the electric field considerably depends on the carrier, temperature, and diameter of the nanowires. In particular, the threshold between the linear and non-linear regimes exhibits important variations. The drift velocity reaches a maximum value and then drops. These trends can be related to the effects of quantum confinement on the band structure of the nanowires. We also discuss the impact of the different phonon modes and show that high-energy phonons can, unexpectedly, increase the drift velocity at a high electric field. © *2015 AIP Publishing LLC*.
[http://dx.doi.org/10.1063/1.4928525]

At a low electric field E, the charge carriers in a semiconductor acquire a finite drift velocity $v = \mu_0 E$, where μ_0 is the mobility. However, at a high electric field, v becomes a sub-linear function of E and eventually saturates when any further kinetic energy gained from the field is lost to the lattice. In bulk Si, the electron velocity saturates at about 10^7 cm/s (at $T = 300$ K) when the carriers in any of the six equivalent conduction band valleys get scattered to another valley by the emission of optical phonons.[1,2] In bulk GaAs, the situation is different because the conduction band features a single low-mass valley at Γ and four heavy-mass valleys at 0.3 eV higher. As a consequence, the velocity continuously increases with the electric field as long as the electrons occupy only the lowest valley but reaches a maximum and then drops considerably once the electrons get scattered to the heavy-mass valleys.[3]

Therefore, the transport properties at the high-electric field depend on the interplay between the different bands or the valleys of a material. This suggests that similar effects could be achieved with quantum confinement. In this letter, we show that ⟨110⟩ oriented Si nanowires (SiNWs) with small diameter that have received significant attention over the last decade[4–9] exhibit remarkable variations in the evolution of the drift velocity with the electric field. For this purpose, we solve the non-linear Boltzmann transport equation (BTE) on top of atomistic electron and phonon band structures.[10–13] We find that the drift velocity in SiNWs first increases at a low electric field, then saturates, and might eventually drop. We predict saturation velocities of electrons and holes smaller than in bulk Si at room-temperature peak below the bulk saturation velocity ($\sim 10^7$ cm/s).[2,14] We relate these trends to the effects of quantum confinement on the band structure of electrons and holes. We also discuss the role of the different phonon modes and show that high-energy phonons can, surprisingly, increase the drift velocity at a high electric field.

Modeling high-field transport is a difficult task, which is usually achieved by using Monte Carlo methods in the bulk Si[2,14] and Si layers.[15–17] In the latter case, confined subbands are usually computed in the envelope function approximation. More recently, Monte Carlo simulations have been performed on SiNWs using tight-binding (TB) band structures.[12] All these calculations, however, assume that the carriers are coupled to the bulk phonons. Yet, recent studies on the low-field transport in small diameter SiNWs, based on fully atomistic descriptions of the electrons and phonons,[18–21] have shown that the carriers couple in a complex manner to many phonon modes due to the strong confinement. At the high field transport, the situation is even worse because, in principle, the hot carriers have enough energy to excite phonons in the whole spectrum. Therefore, our aim in the present work is to explore the high-field transport taking all the possible electron-phonon scattering processes into account.

Unlike previous theoretical works that used the Monte Carlo method to solve the BTE, we use MINPACK, a non-linear equation solver, in order to compute the distribution function directly. Under a homogeneous electric field E, the distribution function f_{ik} of band i at a k-point k is the solution of the BTE

$$\frac{-eE}{\hbar}\nabla_k f_{ik} = \sum_{jk' \neq ik} \left[W_{ik,jk'} f_{ik}(1 - f_{jk'}) - W_{jk',ik} f_{jk'}(1 - f_{ik}) \right]. \tag{1}$$

The scattering rates $W_{ik,jk'}$ are calculated with the same methodology as in our previous works on the low-field transport.[19,21] The electronic band structure and wave functions are self-consistently computed with a $sp^3d^5s^*$ TB model on a regular grid of 1024k points.[11,22] We assume a gate-all-around

a)Electronic mail: yniquet@cea.fr
b)Electronic mail: christophe.delerue@isen.fr

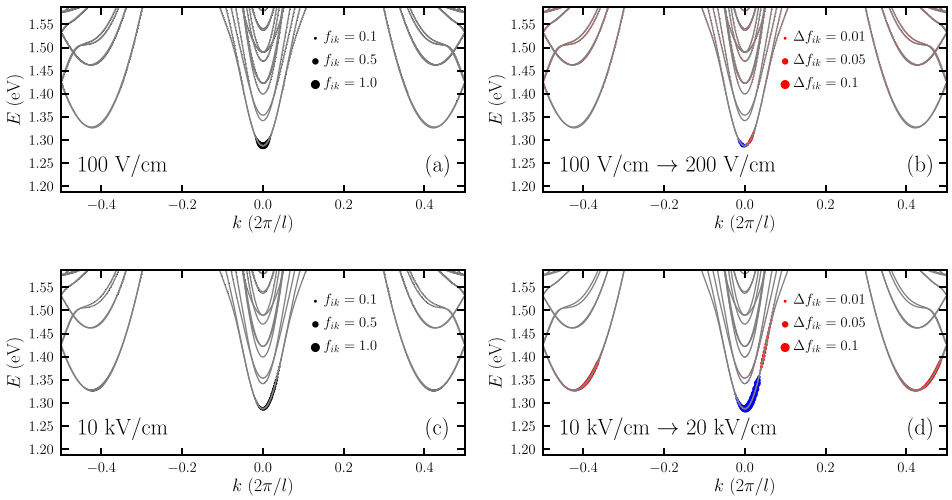

FIG. 1. Conduction band structure of a ⟨110⟩-oriented, 5 nm diameter SiNW (gray lines). The distribution function f_{ik} at $T = 77$ K calculated for an electric field $E = 100$ V/cm (a) and $E = 10$ kV/cm (c) is represented by the size of the black dots. (b) and (d) Same but the size of the dots represents the change Δf_{ik} in the electron distribution function when increasing E from 100 to 200 V/cm (b), and from 10 to 20 kV/cm (d). (b) and (d) Blue dots indicate a decrease in the distribution function and red dots an increase.

configuration with a 2 nm thick HfO_2 gate oxide and a target charge density $n = \sum_{ik} f_{ik}/l = 10^6$ cm^{-1} (where l is the length of the unit cell). The phonon band structure and wave functions are calculated with a Valence Force Field model.[23] The carrier-phonon scattering rates are computed with Fermi's Golden rule[19] for all phonon modes and all electronic states at 1 eV from the conduction or valence band edge. The gradients $\nabla_k f_{ik}$ are evaluated numerically. These coupled equations are then solved exactly using MINPACK. The drift velocity is finally given by $v = \sum_{ik} f_{ik} v_{ik} / \sum_{ik} f_{ik}$.

The conduction band structure of a ⟨110⟩-oriented, 5 nm diameter SiNW is plotted in Fig. 1. There are two kinds of valleys: Low energy and low mass Z valleys at $k = 0$ ($m^* \sim m_t^* = 0.19\, m_0$), and larger mass X, Y valleys above 42 meV at $k = \pm 0.42 \times 2\pi/l$ ($m^* \sim m_l^* = 0.92\, m_0$). This behavior results from the strong anisotropy of the conduction band of the bulk Si.[11] Both kinds of valleys are fourfold degenerate (with spin).

Fig. 1 shows the variations of the distribution function in this SiNW at $T = 77$ K. f_{ik} departs from Fermi-Dirac statistics, which results from the balance between carrier acceleration by the electric field and carrier scattering by the phonons. At the low electric field (Fig. 1(a)), the distribution function still looks (almost) symmetric with respect to the conduction band minima (CBMs); yet, the electric field accelerates and drags the electrons from the negative to positive group velocity states (Fig. 1(b)). Some of these electrons are backscattered to the negative group velocity states by the phonons, and that is why the variations of the distribution function are not symmetric with respect to the CBMs in Fig. 1(b). At the high electric field, the distribution function is clearly asymmetric with respect to the CBMs (Fig. 1(c)), most of the electrons being accelerated in the positive group velocity states. A few of the electrons are, however, transferred from the low mass valleys at $k = 0$ to the heavy mass valleys at $k = \pm 0.42 \times 2\pi/l$ (Fig. 1(d)).

The drift velocity v and the effective mobility $\mu(E) = v/E$ are plotted as a function of the electric field E in Fig. 2(a), for 2 and 5 nm diameter SiNWs at $T = 77$ K and $T = 300$ K, respectively. As shown in Fig. 1, the drift velocity at $T = 77$ K increases linearly with the field at first, then saturates, and eventually drops due to the valley transfer. However, the temperature widens the distribution function and smoothens out the effects of valley transfer, which are hardly visible in the 5 nm diameter SiNW at room temperature.

In general, the drift velocity in the saturation regime is comparable but is smaller than that of the bulk Si. At $T = 300$ K, the drift velocity is $v = 0.74 \times 10^7$ cm/s at $E = 10^5$ V/cm in the 5 nm diameter SiNWs, which is below the bulk value

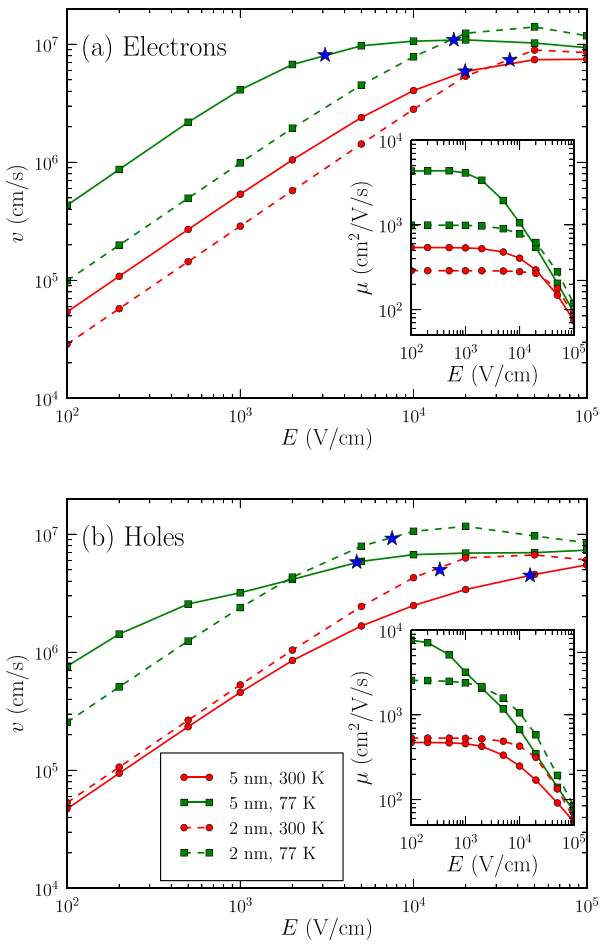

FIG. 2. Drift velocity and effective mobility of electrons (a) and holes (b) as a function of the electric field in ⟨110⟩ SiNWs with a diameter of 2 nm (dashed line) and 5 nm (solid line) at $T = 77$ K (green lines with square markers) and $T = 300$ K (red lines with dot markers), respectively. The blue stars on each curve indicate the threshold field E_{sat}. In the bulk Si, $E_{sat} \sim 1.5 \times 10^4$ V/cm for electrons and $E_{sat} \sim 4 \times 10^4$ V/cm for holes at room temperature.[2]

($\sim 10^7$ cm/s). This reduction may be explained by the stronger electron-phonon interactions in SiNWs.[19,21] As in the bulk Si, the drift velocities near the saturation slightly increase with the decrease in temperature, reaching $v = 0.94 \times 10^7$ cm/s at $E = 10^5$ V/cm and $T = 77$ K.[2]

We can define a threshold field E_{sat} for the saturation regime as the lowest field such that $v > 0.8 v_{max}$ (where v_{max} is the peak velocity). E_{sat} is indicated as a star in Fig. 2. Since the low-field mobility μ_0 is much more dependent on the diameter and temperature than v_{max}, wires with larger mobility μ_0 exhibit lower $E_{sat} \sim 0.8 v_{max}/\mu_0$, i.e., the effective mobility starts to degrade at lower field (inset of Fig. 2(a)). μ_0 is actually smaller in the 2 nm SiNW than in the 5 nm diameter SiNW because of the enhancement of the electron-phonon interactions with decreasing diameter.

We now turn to the case of holes. Quantum confinement in SiNWs splits heavy- and light-hole bands.[11,21] In ⟨110⟩ SiNWs, the highest sub-bands have a strong light-hole character. For example, in a 5 nm diameter NW, the first heavy hole sub-band is the fourth one, so that the splitting between heavy- and light-hole sub-bands is about 46 meV (Fig. 3). The evolution of the distribution function of holes with respect to the electric field is similar to that of electrons. Fig. 1(d) shows that the holes can be transferred from the top light-hole to the nearby heavy-hole sub-bands at a very high electric field. The drift velocity and the effective mobility of the holes are plotted as a function of the electric field in Fig. 2(b). At $E = 10^5$ V/cm, the drift velocity is $v = 0.56 \times 10^7$ cm/s at $T = 300$ K and $v = 0.75 \times 10^7$ cm/s at $T = 77$ K for a 5 nm diameter SiNW. It is slightly smaller than the drift velocity of electrons, although similar saturation velocities are expected for electrons and holes in the bulk Si (around 10^7 cm/s).[2]

Fig. 4 shows the phonons that actually limit the drift velocity in a 5 nm diameter SiNWs. Here we plot $\mu(\hbar\omega)$, the mobility accounting for phonons with the energy below $\hbar\omega$ only. In the bulk Si, the holes are mostly coupled to the acoustic phonons and to the LO/TO branches near Γ ($\hbar\omega \sim 62$ meV). In the case of electrons, the *f*-type inter-valley scattering (e.g., $X \rightarrow Y, Z$) is dominated by phonons with energies around 19, 47, and 59 meV, while the *g*-type inter-valley scattering (e.g., $+Z \rightarrow -Z$) is dominated by phonons with energies around 12, 19, and 62 meV. As shown in Figs. 4(a) and 4(b), the active phonon modes in SiNWs belong to the same categories but can be distributed in

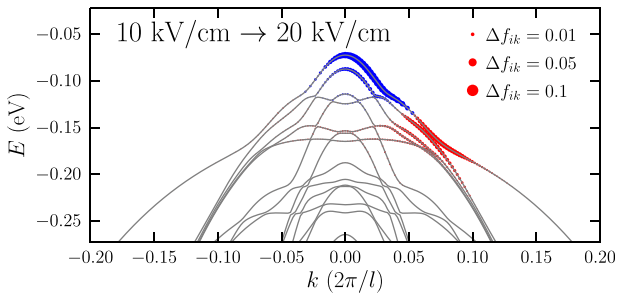

FIG. 3. Valence band structure of a ⟨110⟩-oriented, 5 nm diameter SiNW (gray lines). The size of the dots represents the change in the hole distribution function when increasing the electric field from 10 to 20 kV/cm at $T = 77$ K. Blue dots indicate a decrease in the occupation probability and red dots an increase.

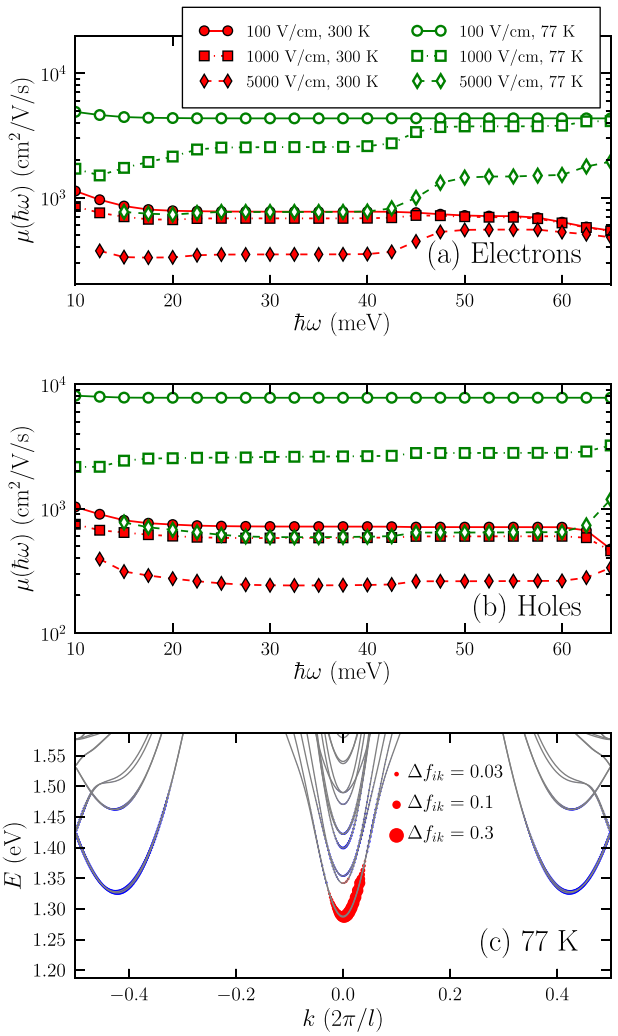

FIG. 4. $\mu(\hbar\omega)$ calculated for electrons (a) and holes (b) in a ⟨110⟩-oriented, 5 nm diameter SiNW. $\mu(\hbar\omega)$ is the mobility accounting for phonons with energy below $\hbar\omega$ only [hence the total phonon-limited mobility is $\mu(\hbar\omega > 65$ meV)]. The results are shown for $E = 100$, 1000, and 5000 V/cm, and for $T = 77$ K (green lines with open symbols) and $T = 300$ K (red lines with filled symbols). (c) The change of the electron distribution function at $E = 5000$ V/cm and $T = 77$ K when increasing the limit of phonon energies from 42.5 to 65 meV. Blue dots indicate a decrease of the distribution function and red dots an increase.

slightly broader ranges because the selection rules are partially lifted by confinement. Also, the role of the different modes is strongly dependent on the temperature and electric field. At $T = 77$ K, the carriers are mostly scattered by acoustic phonons at the low electric field $E = 100$ V/cm.[19] The distribution function, however, widens with increasing electric field, which enhances acoustic phonon scattering and opens paths for spontaneous optical phonon emission. Interestingly, the mobility at the high electric field can increase when more phonons are taken into account, which is rather counter-intuitive. This is because the emission of high-energy phonons brings electrons back to the bottom of the low-mass *Z* valleys at $k = 0$, which limits valley transfer by the electric field and low-energy phonons, as shown in Fig. 4(c). Likewise, the emission of high-energy phonons packs holes in the top light-hole bands and limits the population of the heavy-hole bands. At room temperature, all phonons have sizeable effect whatever be the field. Yet, the high energy phonons backscatter

carriers in the lowest sub-bands and limit the mobility at the low electric field, while they again hinder valley transfer and increase the drift velocity at the high electric field.

In order to have a deeper understanding of this behavior, we have also performed Non-Equilibrium Green's Functions calculations[24] on a model system. We have considered electrons in either parabolic (effective mass) or non-parabolic (two-bands[25] $\mathbf{k}\cdot\mathbf{p}$) bands, with dispersionless acoustic phonons, and the above three *f* and three *g* inter-valley processes. These simulations confirm that the high-energy *g*-type phonons on top of the acoustic and *f*-type phonons can have a beneficial impact on the carrier velocity. This effect is enhanced by the strong non-parabolicity of the *Z* valleys at $k=0$, since the emission of high-energy phonons from a quasi-linear band does not result in a significant slow down of the carriers.

In conclusion, we have shown that the quantum confinement in ⟨110⟩ SiNWs alters the relationship between the drift velocity of carriers and the electric field in a considerable manner. The drift velocity indeed reaches a non-linear regime at a threshold field which depends on the charge carrier, the temperature, and the diameter of the nanowires. Above that threshold field, the drift velocity can exhibit a peak instead of a straight saturation as in the bulk Si due to a valley transfer effect. Strikingly, scattering by high-energy phonons can limit that valley transfer and actually increase the drift velocity at the high electric field. In spite of these differences, the drift velocity at $E=10^5$ V/cm is only slightly smaller in SiNWs than in bulk Si. These trends can be related with the effects of the confinement on the band structure of the nanowires.

This work was supported by the French National Research Agency (ANR) project "NOODLES" ANR-13-NANO-0009-02. The calculations were run on the TGCC/Curie machine using allocations from GENCI and PRACE.

[1]E. Conwell, in *Solid State Physics*, edited by D. Turnbull and H. Ehrenreich (Academic Press, New York, London, 1967), Vol. 9.
[2]C. Jacoboni, C. Canali, G. Ottaviani, and A. A. Quaranta, Solid State Electron. **20**, 77 (1977).
[3]C. Jacoboni and L. Reggiani, Adv. Phys. **28**, 493 (1979).
[4]D. D. D. Ma, C. S. Lee, F. C. K. Au, S. Y. Tong, and S. T. Lee, Science **299**, 1874 (2003).
[5]Y. Wu, Y. Cui, L. Huynh, C. J. Barrelet, D. C. Bell, and C. M. Lieber, Nano Lett. **4**, 433 (2004).
[6]J. Goldberger, A. I. Hochbaum, R. Fan, and P. D. Yang, Nano Lett. **6**, 973 (2006).
[7]N. Singh, A. Agarwal, L. Bera, T. Liow, R. Yang, S. Rustagi, C. Tung, R. Kumar, G. Lo, N. Balasubramanian, and D.-L. Kwong, IEEE Electron Device Lett. **27**, 383 (2006).
[8]K. Trivedi, H. Yuk, H. C. Floresca, M. J. Kim, and W. Hu, Nano Lett. **11**, 1412 (2011).
[9]R. Lavieville, F. Triozon, S. Barraud, A. Corna, X. Jehl, M. Sanquer, J. Li, A. Abisset, I. Duchemin, and Y.-M. Niquet, Nano Lett. **15**, 2958 (2015).
[10]C.-Y. Yeh, S. B. Zhang, and A. Zunger, Phys. Rev. B **50**, 14405 (1994).
[11]Y. M. Niquet, A. Lherbier, N. H. Quang, M. V. Fernández-Serra, X. Blase, and C. Delerue, Phys. Rev. B **73**, 165319 (2006).
[12]A. Verma, A. K. Buin, and M. P. Anantram, J. Appl. Phys. **106**, 113713 (2009).
[13]R. Rurali, Rev. Mod. Phys. **82**, 427 (2010).
[14]G. Ottaviani, L. Reggiani, C. Canali, F. Nava, and A. Alberigi-Quaranta, Phys. Rev. B **12**, 3318 (1975).
[15]M. Fischetti, IEEE Trans. Electron Devices **38**, 634 (1991).
[16]C. Jungemann, A. Emunds, and W. Engl, Solid State Electron. **36**, 1529 (1993).
[17]L. Lucci, P. Palestri, D. Esseni, and L. Selmi, Solid-State Electron. **49**, 1529 (2005).
[18]M. Luisier and G. Klimeck, Phys. Rev. B **80**, 155430 (2009).
[19]W. Zhang, C. Delerue, Y.-M. Niquet, G. Allan, and E. Wang, Phys. Rev. B **82**, 115319 (2010).
[20]M. Luisier, Appl. Phys. Lett. **98**, 032111 (2011).
[21]Y. M. Niquet, C. Delerue, D. Rideau, and B. Videau, IEEE Trans. Electron Devices **59**, 1480 (2012).
[22]Y. M. Niquet, D. Rideau, C. Tavernier, H. Jaouen, and X. Blase, Phys. Rev. B **79**, 245201 (2009).
[23]D. Vanderbilt, S. H. Taole, and S. Narasimhan, Phys. Rev. B **40**, 5657 (1989).
[24]Y.-M. Niquet, V.-H. Nguyen, F. Triozon, I. Duchemin, O. Nier, and D. Rideau, J. Appl. Phys. **115**, 054512 (2014).
[25]V. Sverdlov, G. Karlowatz, S. Dhar, H. Kosina, and S. Selberherr, Solid-State Electron. **52**, 1563 (2008).